

Lattice Anharmonicity in Defect-Free Pd Nanowhiskers

Lisa Y. Chen,¹ Gunther Richter,² John P. Sullivan,³ and Daniel S. Gianola¹

¹*Department of Materials Science and Engineering, University of Pennsylvania, Philadelphia, Pennsylvania 19104, USA*

²*Max-Planck-Institut für Intelligente Systeme, D-70589 Stuttgart, Germany*

³*Sandia National Laboratories, Albuquerque, New Mexico 87185, USA*

(Received 25 May 2012; published 18 September 2012)

We have investigated anharmonic behavior of Pd by applying systematic nanoscale tensile testing to near defect-free nanowhiskers offering a large range of elastic strain. We measured size-dependent deviations from bulk elastic behavior in nanowhiskers with diameters as small as ~ 30 nm. In addition to size-dependent variations in Young's modulus in the small strain limit, we measured nonlinear elasticity at strains above $\sim 1\%$. Both phenomena are attributed to higher-order elasticity in the bulklike core upon being biased from its equilibrium configuration due to the role of surface stresses in small volumes. Quantification of the size-dependent second- and third-order elastic moduli allows for calculation of intrinsic material nonlinearity parameters, e.g., δ . Comparison of the size-independent values of δ in our nanowhiskers with studies on bulk fcc metals lends further insight into the role of length scales on both elastic and plastic mechanical behavior.

DOI: [10.1103/PhysRevLett.109.125503](https://doi.org/10.1103/PhysRevLett.109.125503)

PACS numbers: 62.25.-g, 62.20.D-, 62.23.Hj, 68.35.Gy

Nonlinear elasticity in crystalline materials is directly tied to lattice anharmonicity owing to large deviations in interatomic separation from the equilibrium values. Several important material properties are defined by this anharmonic regime, including thermal expansion [1–3], phonon interactions [1,4,5], and temperature and pressure dependence of elastic constants [6–8]. Measurements of anharmonicity in bulk materials have often been performed through ultrasound velocity measurements or micro-whisker tensile testing, the latter of which requires the introduction of large stresses. Consequently, such experiments have been limited by the onset of plastic relaxation mechanisms at low stresses in these systems [9]. Recent advances in mechanical testing allow for investigating the response of nominally defect-free crystalline nanostructures in which stresses near theoretically predicted levels are required for plasticity to occur [10–12], although rarely has nonlinear elasticity's role at the nanoscale been addressed. Nanoscale volumes comprising large fractions of miscoordinated atoms residing at surfaces and interfaces are expected to play an increasingly important role in deformation behavior. Nanostructures such as thin films and nanowires are often modeled as composites of atomically miscoordinated surfaces (and edges) encompassing a bulklike core; therefore, it should be expected that the relative contributions of surface and bulk effects on elastic behavior are roughly correlated to the surface-to-volume ratio [13–15]. In investigating material properties at the nanoscale, observed deviations from bulk behavior are often analyzed only within the framework of surface contributions such as residual surface stresses and surface stiffness, both of which are attributed to the reduced electron density at the surface [16–19]. In the presence of residual stresses in the surface, some change in the core

must take place to balance these stresses at equilibrium, but these changes and thereby the contributions of the modified core are often overlooked.

Using a combination of defect-free metallic nanowires and *in situ* mechanical testing, we have measured nonlinear mechanical response at applied axial strains in excess of 1% that is completely reversible. By analyzing the size dependence of the second and third-order elastic moduli, we deduce a size-independent nonlinearity parameter, which allows for direct comparisons to lattice anharmonicity in bulk fcc metals. Our pristine nanoscale crystals and systematic testing approach provide results of both nanoscale mechanical phenomena and bulk behavior beyond the limit accessible by conventional macroscopic methods.

The single-crystalline Pd nanowhiskers (NWs) examined in this study were grown by thermal evaporation onto a SrTiO₃-coated Si substrate under ultrahigh vacuum conditions at elevated temperature ($T \sim 1200$ °C). Further details of the fabrication process can be found elsewhere [20,21]. A representative transmission electron microscopy (TEM) image of an as-grown NW, as shown in Fig. 1(a) confirms that the wires are single-crystalline and free of defects visible in TEM, such as dislocations or vacancy aggregates. Pd is not known to form a stable oxide unless exposed to an oxygen environment at elevated temperatures [22–24]. We confirm the absence of surface oxide with high resolution scanning TEM, although a thin layer of carbon-based deposit from imaging is often observed. The NW axes are oriented along $\langle 110 \rangle$ directions [Fig. 1(a) inset] and possess high aspect ratios, with lengths $5 < l < 20$ μm and diameters $30 < d < 150$ nm. Individual nanowires were manipulated in a scanning electron microscope (SEM) and mounted to a MEMS tensile testing stage via

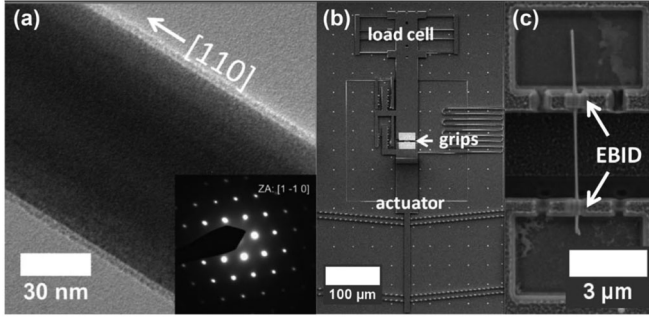


FIG. 1. (a) TEM image and SAED diffraction pattern (inset) for a sample Pd NW. (b) Thermally actuated tensile testing stage onto which NWs are manipulated. The comb features to the side of the sample grips may be used for tracking displacements of the load cell and actuator. (c) Pd NW across the testing grips.

Pt-based electron-beam induced deposits (EBID) [25]. Actuation of the testing device is achieved by Joule heating-induced thermal expansion of polysilicon chevron beams, with heat flow to the sample mitigated by a SiN_x strip. Force on the specimen is deduced by directly measuring displacements of compound flexure beams of polysilicon on the opposite grip. *In situ* tensile tests were performed at room temperature and nominal strain rates $\sim 10^{-4} \text{ s}^{-1}$ in both a SEM and an optical microscope, with most specimens tested elastically in both environments to assure consistent results. Digital image correlation (DIC) [26] of image sequences obtained during testing was used to measure the displacements relative to fixed points on the substrate, which are converted to specimen stress and strain. Select experiments, where EBID markers were deposited along the length of nanowhiskers, were employed to facilitate direct strain measurement and showed good agreement with strain deduced from relative grip displacements, demonstrating negligible compliance of the gripping material. (See Supplemental Material [27]).

The stress-strain behavior for all Pd NWs was characterized by linear elastic behavior at strains $< 1\%$ and clear nonlinearity at larger strains. Systematic unloading beyond the linear (Hookean) regime showed the deformation path to follow the nonlinear loading curves and return to zero strain, indicating elastic behavior. Figure 2(a) shows representative load-unload stress-strain curves for two nanowhiskers with different diameters (110 and 33 nm) as well as subsequent loading curves to fracture. Nonlinear elastic behavior was measured to occur at strains as high as $\sim 5\%$ and stresses in excess of 4 GPa. Some specimens displayed plastic deformation preceding fracture, which could be clearly distinguished from the elastic regime [e.g., 33 nm specimen shown in Fig. 2(a)]. We note that measured fracture strengths were as high as 7.1 GPa (corresponding to resolved shear stresses on the $\{111\}/\langle 112 \rangle$ slip system of $\sim 8\%$ of the shear modulus of Pd), which are near estimates of the theoretical shear strength, consistent with other reports of high strength in fcc nanowhiskers [21,28]. To

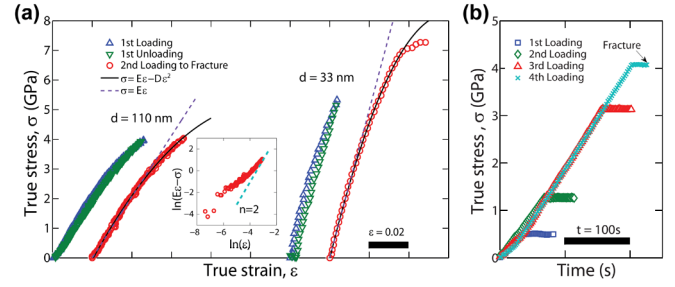


FIG. 2 (color online). (a) Loading, unloading, and subsequent fracture (offset along strain axis for clarity) stress-strain curves for two Pd NWs. Load-unload tests indicate no residual strain in NWs after unloading. Linear and quadratic fits (reconciled by the power law exponent shown in the inset) to the fracture curves are shown. (b) Stress-time data for a representative Pd NW, during which the actuator was held stationary, confirming elastic behavior until near the fracture stress.

confirm the elastic limit of our Pd nanowhiskers, the actuator position was fixed at various increments of strain, and load was measured for ~ 1 min hold periods, as shown in Fig. 2(b). For holds at approximately 0.5, 1.2, and 3.1 GPa, no clear load relaxation was measured, indicating the absence of detectable plastic deformation in this regime of nonlinear mechanical behavior. Measurable load relaxation was only measured at stresses higher than 4 GPa, which directly preceded fracture of the sample. These experiments reveal a large range of elastic strain over which both linear and nonlinear elasticity can be quantified.

The linear elastic response of a material is entirely represented by the quadratic term of the interatomic potential energy, while nonlinear elasticity requires higher-order terms. This translates to the following stress-strain relationship for uniaxial loading

$$\sigma = E\varepsilon + D\varepsilon^2 + \dots \quad (1)$$

where σ is the true stress, ε is the true strain, and E and D are the second-order (Young's) and third-order moduli, respectively. Our data show a quadratic fit to sufficiently capture the nonlinear response until fracture [inset of Fig. 2(a)]. We note that this relationship has been used in evaluating the large-strain elastic response of other nanostructures such as graphene [14,15,29].

The moduli E and D were directly determined for all tested Pd NWs by nonlinear least-squares fitting of the measured tensile response to Eq. (1). D was measured to be negative and with absolute values an order of magnitude larger than E , indicating a strong elastic softening beyond the linear (Hookean) regime. Most notably, both E and D were measured to be size dependent, with increasing absolute values with decreasing NW diameter (Fig. 3). E was measured to be approximately 120 GPa for NWs larger than 100 nm, which is close to the bulk value of Young's modulus in Pd for a $\langle 110 \rangle$ axial orientation (136 GPa) [30], while increasing to ~ 290 GPa in the 33 nm NW [Fig. 3(a)].

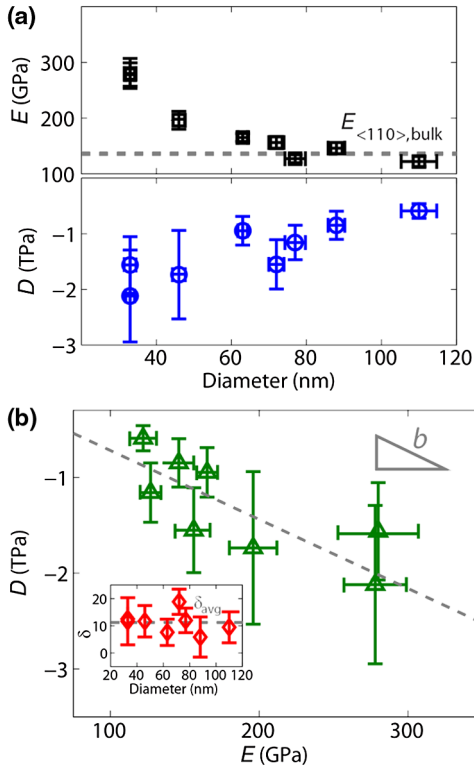


FIG. 3 (color online). (a) E and D obtained from least-squares quadratic fitting, showing a clear dependence of both quantities on NW size. (b) Plotting E vs D demonstrates a linear correlation, suggesting that the slope b , the strain-expanded nonlinearity parameter, is an intrinsic size-independent property. The inset confirms that the nonlinearity parameter δ is not a function of diameter over the tested size range. See Supplemental Material [27] for details on the error analysis.

While the linear response at low strains was shown to stiffen with decreasing size, D was measured to correspondingly decrease (increasing magnitude) [Fig. 3(a)], revealing a more pronounced deviation from linear behavior in the smallest tested NWs.

That both linear and higher-order elastic constants show size dependence is noteworthy. Figure 3(b) shows E and D to be roughly linearly correlated, which suggests that an additional material parameter can be defined that is size independent, and hence, representative of a bulklike quantity. Such an approach can be reconciled by considering the elastic strain energy as a function of interatomic separation during uniaxial loading of our NWs. Following Diao *et al.* [14], by accounting for Poisson contractions, a relationship between Eq. (1) and the strain energy $U(\epsilon)$ of a nanowire with Poisson's ratio ν and initial volume V_0 subjected to uniaxial tension can be expressed as

$$\frac{U(\epsilon)}{V_0} = E \left(\frac{1}{2} \epsilon^2 + \frac{1}{3} (1 - 2\nu + b) \epsilon^3 \right), \quad (2)$$

where $b = D/E$, the so-called strain-expanded nonlinearity parameter. Because $b \propto \partial^3 U / \partial \epsilon^3$ (i.e., related to

third-order elastic constants), a constant b implies a signature of the interatomic behavior of a crystal corresponding to nonlinear behavior in bulk Pd. We measure $b = -7.19 \pm 1.94$; i.e., bulk Pd should elastically soften in tension along the $\langle 110 \rangle$ direction. While experiments of bulk Pd elastic behavior at high strains are not available, molecular statics simulations of higher-order elastic moduli in other bulk fcc metals have been performed [14,15]. Liang *et al.* found that in bulk Cu along the $\langle 110 \rangle$ direction, the instantaneous stress-strain slope decreases ($b_{110} = -9.885$) (agrees with our findings) as well as along $\langle 111 \rangle$ ($b_{111} = -0.587$) but increases for $\langle 100 \rangle$ ($b_{100} = 4.155$) [15]. A similar trend in atomistic simulations of bulk Au was observed by Diao *et al.* where the Young's modulus along the $\langle 100 \rangle$ direction was found to decrease with compressive strain; i.e. b_{100} is positive [14]. Comparing our results with these findings, the response of the tested Pd NWs along the $\langle 110 \rangle$ direction is consistent with predictions for the interatomic behavior of fcc metals. As the magnitude of b is a direct measure of the degree of anharmonicity, one can estimate the anharmonic contribution by considering the relative deviation from a harmonic approximation [1st term of Eq. (2)]. We write a dimensionless expression for the fractional anharmonic contribution to the strain energy density as $2/3(1 - 2\nu + b)\epsilon$. Using $\nu = 0.39$ and our measured value of b for Pd nanowires, this value would be $\sim 5\%$ and $\sim 25\%$ for strains of 0.01 and 0.05, respectively, suggesting that anharmonicity plays a substantial role particularly near the fracture strain.

Further comparisons with nonlinear elastic behavior in fcc metals can be made by expanding in stress rather than strain [31]:

$$\epsilon = \left(\frac{\sigma}{E} \right) + \delta \left(\frac{\sigma}{E} \right)^2. \quad (3)$$

Here, nonlinearity is characterized by the stress-expanded parameter δ , which is a function of both second- and third-order elastic constants [4,31,32]. Using this framework, we measure $\delta = 11.2 \pm 3.9$ for our $\langle 110 \rangle$ Pd NWs [inset of Fig. 3(b)], which, to the best of the authors' knowledge, is the first measurement of δ in Pd. Nevertheless, it is still insightful to compare to δ values obtained in other fcc noble metals [31–34], which are consistent in sign for each low-index orientation (negative for $\langle 100 \rangle$, positive for $\langle 110 \rangle$ and $\langle 111 \rangle$), with the magnitude of δ_{110} usually being the highest (typical values in noble metals range from ~ 8 to ~ 11). Also noteworthy is the qualitative agreement between these experimental studies and the simulations by Diao *et al.* of $\langle 100 \rangle$ Au and by Liang *et al.* in Cu for all three directions [14,15]. Comparing with the current work, our value δ_{110} obtained for Pd is the largest among other fcc metals but consistent in sign and magnitude, suggesting a very large degree of anharmonicity. (See Supplemental Material [27]).

Having shown a direct measurement of the size-independent nonlinearity parameter in Pd along the $\langle 110 \rangle$ direction, we now turn our attention to the size dependence of E and D . Such size dependence in E is commonly attributed to the effect of increasing surface-to-volume ratio in nanostructures via two separate effects. The first is the contribution of a surface layer with distinct elastic properties from the bulk to the total stiffness of a nanostructure, a direct result of the atomic bonding configuration near a free surface [17,35,36]. In this case, the total surface stress along the nanowire axis is often represented as $\tau = \tau_0 + S\varepsilon$, where S is the surface stiffness (or surface elastic modulus) and τ_0 is the surface stress at zero applied strain [19,37]. This contribution of the surface stiffness S leading to the deviation in E from the bulk value E_0 is estimated by $(E - E_0)/E_0 = \alpha(h/h_0)$, where α is a geometric factor, $h_0 = |S/E_0|$, and h is the characteristic length scale of the structure [17,19]. Using surface stiffness values obtained from atomistic simulations [19], we calculated h for several low-energy surfaces ($\{100\}$, $\{110\}$, $\{111\}$, and $\{112\}$) on a $\langle 110 \rangle$ -NW assuming a square $h \times h$ cross-section under tension ($\alpha = 4$). For a 10% difference in apparent E (sufficiently large so as to be measured in our experimental setup), $h < 4$ nm, which is well below where our Pd NWs begin to show deviations from bulk elastic behavior. We note that other experimental and atomistic simulation studies of nanowires also show deviations in E due to surface stiffness at similarly small length scales [37–40]. It is important to recognize that this model assumes a linear elastic response of miscoordinated atoms residing at the surface. Also, to account for changes in stiffness in perfectly coordinated atoms, the surface must be able to affect the response of the fully coordinated core atoms. This can be accomplished by way of a second effect, namely, via surface-stress-induced relaxations [15,41,42]. Changes in bond lengths near the surface can result in large values of τ_0 , which in equilibrium must be balanced by stresses in the material core [19,37,41]. Surface stress effects on the elastic response of nanowires have been extensively modeled [37,38,40,43], but the core stress is often assumed to exhibit linear elastic response. Both Diao *et al.* and Liang *et al.* have found in their simulations that the variations in E with decreasing size in Au and Cu NWs, respectively, can be attributed to higher-order elastic behavior, arising from a surface stress-induced residual stress state along the axial direction of the wire [14,15]. Compressive residual core strains > 0.01 sufficiently shift the initial stress state and thus the apparent E , giving rise to size-dependent elastic behavior. Since we have determined the E and b values for our Pd NWs, we can similarly estimate the residual axial core strain ε_r by using the expression $\varepsilon_r = (E/E_{\text{bulk}} - 1)/2b$ (Fig. 4). This simple approach does not take into account the effects of the surface in the transverse directions, but it does illustrate the significant role the surface may play in

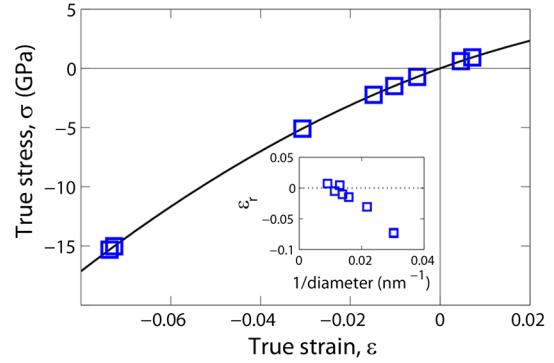


FIG. 4 (color online). Estimation of relaxation strain ε_r along the NW axis. The provided inset shows increasingly compressive relaxation strains for NWs with smaller diameters. The bulk curve for Pd is plotted using the relation in Eq. (1) with $D/E = -7.19$. The anomalous points indicating positive ε_r result from calculations with E values near the bulk value.

evaluating the yield and fracture strength in fcc metal nanostructures.

In conclusion, we have directly measured nonlinear elasticity in $\langle 110 \rangle$ Pd NWs for diameters between approximately 30 and 110 nm and attribute this response to lattice anharmonicity characterized by the nonlinearity parameter δ . This quantity, and likewise its strain-expanded counterpart b , show no size dependence, while the apparent second- and third- order elastic moduli E and D vary with size. The changes in E are attributed to large compressive strains along the axis of the core and highlight the importance of higher-order elastic behavior in evaluating surface stress effects. The correlation between D and E suggests that the size dependence of the third-order elastic modulus is also related to the nonlinear elastic response of the bulklike core. Irrespective of the difference in length scales, the measured nonlinearity of Pd is in general agreement with both atomistic and experimental studies on bulk specimens of other fcc transition metals. This anharmonic behavior not only affects elastic behavior (including temperature dependence) but also is expected to play a significant role in the plastic deformation of defect-free nanostructures. For instance, the large activation entropy contribution to the rate of dislocation nucleation in defect-free fcc metals has been shown to be caused by anharmonic effects such as thermal expansion and thermal softening [44]. By excluding anharmonic effects, calculations for the nucleation rate based on harmonic approximations in transition state theory can err by several orders of magnitude at room temperature, thus affecting predictions of material strength [44,45]. Our results provide a novel method for characterizing size-independent anharmonic bulk properties, not accessible by conventional methods, via size-dependent elastic behavior in defect-free, high-strength nanostructures. The implications of our results extend beyond material elasticity, as the nature of interatomic bonding and vibrations affect mechanical, thermal, electronic, and

physical properties of materials known to be strongly influenced by lattice anharmonicity.

The authors gratefully acknowledge the Penn Regional Nanotechnology Facility and financial support from the National Science Foundation through a CAREER Grant (NSF-DMR 1056293). We thank Erik Bitzek for fruitful discussions and Kate Murphy for technical assistance. This work was performed, in part, at the Center for Integrated Nanotechnologies, a U.S. Department of Energy, Office of Basic Energy Sciences user facility. Sandia National Laboratories is a multiprogram laboratory managed and operated by Sandia Corporation, a wholly owned subsidiary of Lockheed Martin Corporation, for the U.S. Department of Energy's National Nuclear Security Administration under Contract DE-AC04-94AL85000.

-
- [1] Y. Hiki, *Annu. Rev. Mater. Sci.* **11**, 51 (1981).
- [2] Y. Hiki, J. Thomas, and A. Granato, *Phys. Rev.* **153**, 764 (1967).
- [3] J. Thomas, *Phys. Rev.* **175**, 955 (1968).
- [4] A. Seeger and O. Buck, *Z. Naturforsch. Teil A* **15**, 1056 (1960).
- [5] E. F. Lambson, W. A. Lambson, J. E. Macdonald, M. R. J. Gibbs, G. A. Saunders, and D. Turnbull, *Phys. Rev. B* **33**, 2380 (1986).
- [6] C. Weinmann and S. Steinemann, *Phys. Lett. A* **47**, 275 (1974).
- [7] R. Peters, M. Breazeale, and V. Paré, *Phys. Rev. B* **1**, 3245 (1970).
- [8] T. Soma, H. Satoh, and H. Matsuo, *Solid State Commun.* **40**, 933 (1981).
- [9] H. Kobayashi and Y. Hiki, *Phys. Rev. B* **7**, 594 (1973).
- [10] M. A. Haque and M. T. A. Saif, *Exp. Mech.* **43**, 248 (2003).
- [11] D. S. Gianola and C. Eberl, *JOM* **61**, 24 (2009).
- [12] E. P. S. Tan and C. T. Lim, *Rev. Sci. Instrum.* **75**, 2581 (2004).
- [13] H. Park and P. Klein, *Phys. Rev. B* **75**, 085408 (2007).
- [14] J. Diao, K. Gall, and M. L. Dunn, *J. Mech. Phys. Solids* **52**, 1935 (2004).
- [15] H. Liang, M. Upmanyu, and H. Huang, *Phys. Rev. B* **71**, 241403 (2005).
- [16] L. G. Zhou and H. Huang, *Appl. Phys. Lett.* **84**, 1940 (2004).
- [17] R. E. Miller and V. B. Shenoy, *Nanotechnology* **11**, 139 (2000).
- [18] M. Gurtin and A. Ian Murdoch, *Arch. Ration. Mech. Anal.* **57**, (1975).
- [19] V. Shenoy, *Phys. Rev. B* **71**, 094104 (2005).
- [20] G. Richter, *Scr. Mater.* **63**, 933 (2010).
- [21] G. Richter, K. Hillerich, D. S. Gianola, R. Mönig, O. Kraft, and C. A. Volkert, *Nano Lett.* **9**, 3048 (2009).
- [22] W. T. Grubb and L. H. King, *Anal. Chem.* **52**, 270 (1980).
- [23] M. Peuckert, *J. Phys. Chem.* **89**, 2481 (1985).
- [24] E. H. Voogt, A. J. M. Mens, O. L. J. Gijzeman, and J. W. Geus, *Surf. Sci.* **350**, 21 (1996).
- [25] A. Botman, J. J. L. Mulders, R. Weemaes, and S. Mentink, *Nanotechnology* **17**, 3779 (2006).
- [26] C. Eberl, D. S. Gianola, and K. J. Hemker, *Exp. Mech.* **50**, 85 (2008).
- [27] See Supplemental Material at <http://link.aps.org/supplemental/10.1103/PhysRevLett.109.125503> for further details on the testing approach.
- [28] A. Sedlmayr, E. Bitzek, D. S. Gianola, G. Richter, R. Mönig, and O. Kraft, *Acta Mater.* **60**, 3985 (2012).
- [29] C. Lee, X. Wei, J. W. Kysar, and J. Hone, *Science* **321**, 385 (2008).
- [30] J. Rayne, *Phys. Rev.* **118**, 1545 (1960).
- [31] B. Powell and M. Skove, *Phys. Rev.* **174**, 977 (1968).
- [32] F. Milstein and D. Rasky, *Philos. Mag. A* **45**, 49 (1982).
- [33] M. Riley and M. Skove, *Phys. Rev. B* **8**, 466 (1973).
- [34] Y. Hiki and A. Granato, *Phys. Rev.* **144**, 411 (1966).
- [35] C. Chen, Y. Shi, Y. Zhang, J. Zhu, and Y. Yan, *Phys. Rev. Lett.* **96**, 075505 (2006).
- [36] R. C. Cammarata and K. Sieradzki, *Annu. Rev. Mater. Sci.* **24**, 215 (1994).
- [37] F. Song, G. L. Huang, H. S. Park, and X. N. Liu, *Int. J. Solids Struct.* **48**, 2154 (2011).
- [38] R. Dingreville, J. Qu, and M. Cherkaoui, *J. Mech. Phys. Solids* **53**, 1827 (2005).
- [39] M. T. McDowell, A. M. Leach, and K. Gall, *Nano Lett.* **8**, 3613 (2008).
- [40] J.-G. Guo and Y.-P. Zhao, *Nanotechnology* **18**, 295701 (2007).
- [41] G. Yun and H. Park, *Phys. Rev. B* **79**, 32 (2009).
- [42] Z.-J. Wang, C. Liu, Z. Li, and T.-Y. Zhang, *J. Appl. Phys.* **108**, 083506 (2010).
- [43] J. Diao, K. Gall, and M. L. Dunn, *Nature Mater.* **2**, 656 (2003).
- [44] S. Ryu, K. Kang, and W. Cai, *Proc. Natl. Acad. Sci. U.S.A.* **108**, 5174 (2011).
- [45] L. D. Nguyen, K. L. Baker, and D. H. Warner, *Phys. Rev. B* **84**, 024118 (2011).